AMORPHOUS-SILICON MODULE INTERCELL CORROSION

G. R. Mon and R. G. Ross, Jr.
Jet Propulsion Laboratory, Pasadena, CA 91109

ABSTRACT

Three non-electrochemical, moisture-induced a-Si module degradation modes have been observed and their mechanisms studied: (1) the formation and growth of pinholes in the thin-film layers; (2) the directional interfusion of pinholes along process scribe lines to form metallization-free regions that tend to open-circuit the module; and (3) worm-like filiform corrosion in the aluminum layer. The dependency on time-of-exposure to moist environments of the amount of material erosion in the module intercell zone has been quantified by two methods--directly by EDS analysis, and indirectly by sheet resistivity measurements on fully aluminized back surface modules. In addition, changes in maximum power output, series resistance, and open circuit voltage have been documented. Consequences for fielded modules are discussed.

INTRODUCTION

A much-studied and by now well-known amorphous-silicon module instability factor is the Staebler-Wronski effect[1]. Macroscopically, the effect manifests as a loss of efficiency due to fill factor decay. The effect is reversible in that annealing will restore module efficiency to nearly its original value[2].

An equally well-known module reliability problem is corrosion; it manifests as loss of power output and increase of series resistance[3,4]. The types of corrosion directly affecting the performance of amorphous-silicon (a-Si) and crystalline-silicon (C-Si) photovoltaic devices include electrochemical corrosion and galvanic corrosion. Electrochemical corrosion results from applied voltage differentials between different module parts (e.g., cell and frame in C-Si modules), while galvanic corrosion results from self-generated potential differences between contacting conductors (as, for instance, between the back-cell metallization and the transparent conductive oxide (TCO) layer in adjacent cells of a-Si modules).

Electrochemical corrosion in both C-Si and a-Si modules has been well documented[5,6]. Galvanic corrosion is less well understood. It results from direct contact between conductive parts of a module; hence it is not driven by light-generated potentials and may occur day or night. The major concern is that corrosion may open-circuit the a-Si module. This is most likely to result from loss of the conductive oxide layer and/or the contact metallization in the "parasitic cell" region between two adjacent active cells, Fig. 1. Of particular concern are anticipated losses of conductive oxide in regions B, C and D, and of back-surface metallization in regions D, E and F. Some module manufacturers use a conductive filler, such as silver paste, in region D to enhance intercell conductivity; this

Proceedings of the American Institute of Physics
Conference on Stability of Amorphous Silicon
Alloy Materials and Devices
Palo Alto, CA, January 28-30, 1987

practice adds an additional galvanic couple to which the above concern extends.

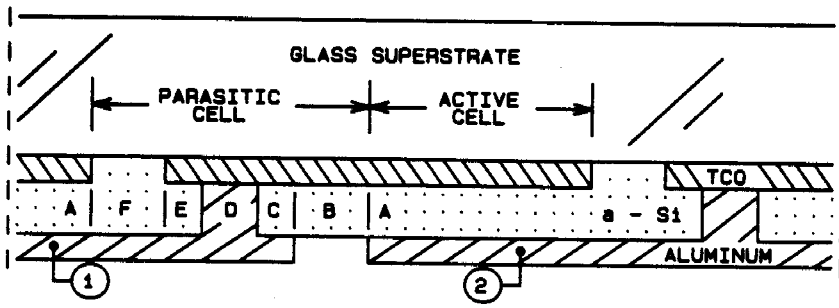

Fig. 1. Series-Connected Thin-Film Cells

A tendency toward open-circuiting will cause increases in contact resistance between the conductive oxide and the rear surface metallization. If this resistance (R_C in Fig. 2) should become too large, the diode characteristic of the parasitic cell will evidence itself as an upward curvature in the active cell's fourth-quadrant I-V characteristic, a reduction of V_{OC}, and loss of maximum power output as a result of the forward drop of the parasitic diode[7].

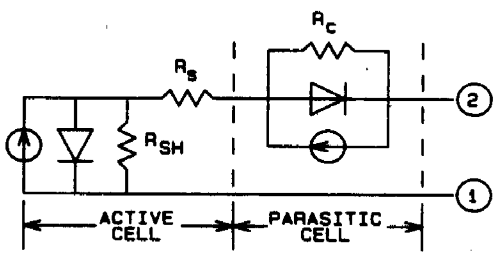

Fig. 2. Equivalent Circuit

A loss of contact metallization has indeed been observed both for unencapsulated and EVA-encapsulated modules, and the losses are in fact most pronounced in the contact scribe zone (region D, Fig. 1). The relatively larger losses that occur in this region are attributable to high mechanical stresses induced in the metallization at the sharp corners formed in the laser scribing of the a-Si layer. Other observed degradation patterns include extensive pinhole formation in the aluminum layer and in the combined aluminum and a-Si layers (and perhaps even the conductive oxide layer), and filiform corrosion in the aluminum layer. The study of these degradation processes and their consequences for a-Si module performance, are described in the remainder of this paper.

EXPERIMENTAL APPROACH

Four separate but related experiments were undertaken to ascertain the non-electrochemical corrosion aspects of a-Si modules. In the first experiment, a number of unencapsulated a-Si modules was exposed for variable intervals to controlled 85°C/100%Rh chamber conditions over an extended period of time. Prior to exposure, and after each exposure interval, these samples were removed from the oven and dark I-V curve data were acquired. From these data, progressive series resistance values were obtained. In addition, photomicrographs of the intercell regions of select samples were obtained using a scanning electron microscope (SEM), and atomic concentration profiles of the intercell region were obtained using energy dispersive X-ray (EDS) techniques. Optical photographs of the intercell region were also obtained.

The exposure times and experimental measurement techniques employed on the second batch of a-Si modules were similar to those used on the first, with the exception that light I-V curve data rather than dark I-V curve data were obtained.

The experimental approach employed for the third batch of samples was as for the first batch except that during exposure the samples in the third batch were forward voltage (reverse current) biased at 3/4-volt differential per cell, approximately equivalent to that experienced during exposure to light. It is known[8] that forward bias conditions stress the a-Si in a manner equivalent to light exposure. This phase of the experiment, then, focussed on differentiating galvanic and other corrosions from the light induced Staebler-Wronski effect.

A fourth set of samples featured a-Si modules encapsulated in the polymer ethylene vinyl acetate (EVA) and then subjected to an exposure and I-V curve acquisition program similar to that for Batch 1 and 2 samples.

When in the course of interpreting the data it became clear that loss of back surface (Al) metallization was a major degradation mode, a fifth batch of samples was subjected to both 85°C/85%RH and 85°C/100%Rh environments. The samples in this batch consisted of thin-film modules featuring fully metallized back surfaces (no break in the aluminum layer). After successive exposures, the sheet resistance of the aluminum layer was measured, using a Kelvin (four-point) probe apparatus, to detect expected increases in surface resistivity values.

Batch identification and pertinent sample and measurement characterization is provided in Table 1.

SAMPLE BATCH	ENVIRONMENT (°C/%RH)	MODULE CHARACTERIZATION	DATA
1	85/100	U	D,X,P
2	85/100	U	L,P
3	85/100	U,FB	D,P
4	85/100	E	L,D,P
5	85/85 85/100	M,E,U	R,P

U = unemcapsulated
E = encapsulated
FB = forward bias
M = full back metallization

D = dark I-V
L = light I-V
X = EDS
P = photos
R = Al sheet resistivity

Table 1. Experimental Parameters

The rationale of this experimental approach is that each sample be exposed to as little light as possible so as to allow an unequivocal differentiation of light-induced instability effects from corrosion degradation. Unfortunately, some exposure to light was necessary, particularly during photography and light I-V curve data acquisition sessions. Exposure during photography, although relatively intense, was generally localized and was never for more than a few minutes. LAPSS exposure during I-V curve data acquisition was at a level of one sun for a period of no more than a few milliseconds and is not considered to be detrimental.

EXPERIMENTAL RESULTS AND DISCUSSION

The rapid deterioration of a-Si module I-V characteristics resulting from exposure to moist environments has been previously demonstrated[5,8] and reconfirmed in these experiments. The most striking observation is the very visually obvious loss of material from the aluminum and a-Si layers of the exposed modules. Such material losses manifest in three forms: (1) as pinholes in either the aluminum layer or in the aluminum and a-Si layers (or perhaps even in all layers) that form and enlarge in time, Fig. 3; (2) as continuous regional losses that can occur anywhere but are apparently more likely to occur along the scribe, etch, and mask lines, Fig. 4; and (3) as wormy lines of aluminum loss that we call filiform corrosion, Fig. 5.

Pinholes (Fig. 3) form in the manner of blisters, most likely at sites of localized contamination on, or defects within, the thin-film layers. Moisture penetrates the layers and chemically reacts at such sites to weaken or destroy the interlayer bonds. Surface tension stress-relieves the uplifted mater-material and opens the blister to form the pinhole. Continued exposure expands the periphery of the pinhole by processes of continual bond breaking and stress relief.

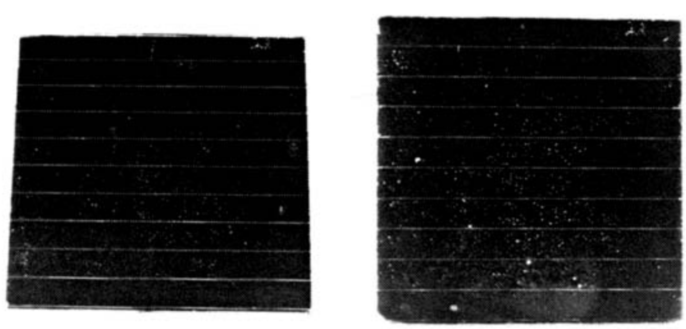

191 hrs 1913 hrs

Fig. 3. Formation and Enlargement of Pinholes, 85°C/100% RH

Material losses in the intercell region (Fig. 4) occur in a similar fashion. But here pinholes tend to form, aggregate, and interfuse along the sharp edges of the various scribe, etch, and/or mask lines. These zones in the thin-film layers are highly prestressed by the various forming processes and provide a directional bias along which material losses occur. This form of material degradation is most detrimental to a-Si module performance as it results in a tendency to open-circuit the module. This phenomenon is clearly evident not only in Fig. 4 but also in Fig. 3, wherein aluminum back-surface metallization loss along the copper bussbar edges have open-circuited the module.

Unlike the highly directional scribe line corrosion described above, filiform corrosion (Fig. 5) proceeds in more random directions within the aluminum layer. Filiform corrosion combines the elements of pinhole formation and stress corrosion cracking: hydrochemical effects weaken the bond of the aluminum layer to its substrate, and stress-relieving in the weakened aluminum bond layer drives the cracking process. The crack front opens perpendicularly to the direction of the normal plane stresses acting upon it, but the direction of crack propagation is along lines of maximum shear stresses, which makes a 45^{o} angle with the direction of maximum tensile stresses. This is why this type of corrosion tends to occur in spiral patterns[5].

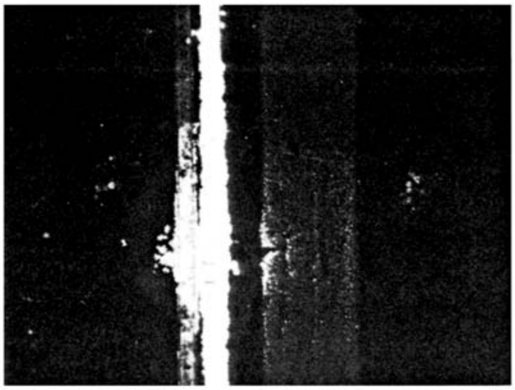

Fig. 4. Material Losses in the Intercell Region

Filiform corrosion, which requires oxygen[9], occurs in the aluminum layer, with which atmospheric oxygen interacts. The phenomenon is not observed in a-Si because the oxygen molecule, even if it can penetrate the aluminum layer and any underlying diffusion barrier, is relatively non-reactive with a-Si--even in the presence of moisture.

Material losses in the intercell zone of a-Si modules has been quantified by means of EDS analysis. EDS profiles were monitored to seek evidence for species concentration changes (chemical reactions, material erosion, etc.). The bar graphs in Fig. 6, showing changes with time of exposure of fractional elemental concentrations in the regions D, E, and F (Fig. 1) in the intercell zone of a typical module substantiate the visual observation of aluminum losses in a region critical to module performance. Loss of conductive oxide in region "B" will also critically impact module performance, but only a-Si losses were observed in this region.

Fig. 5. Stress Corrosion Cracking

Resistivity increases with loss of metallization have been quantified by four-point probe resistance measurements on 5-cm.-wide strips cut from fully aluminized back surface modules. These modules suffered extensive progressive loss of aluminum over large portions of their back surfaces (Fig. 7), perhaps by the formation and flaking of oxide powder, but the resistivity measurements were confined to regions where such losses had not yet occurred. The intent was to quantify aluminum loss rate in the intercell zones by monitoring sheet resistivity increases. A plot of resistivity versus exposure time (Fig. 8) reveals that encapsulation does not effectively prevent aluminum micro-losses in the intercell zone, to which measured resistivity increases are attributed.

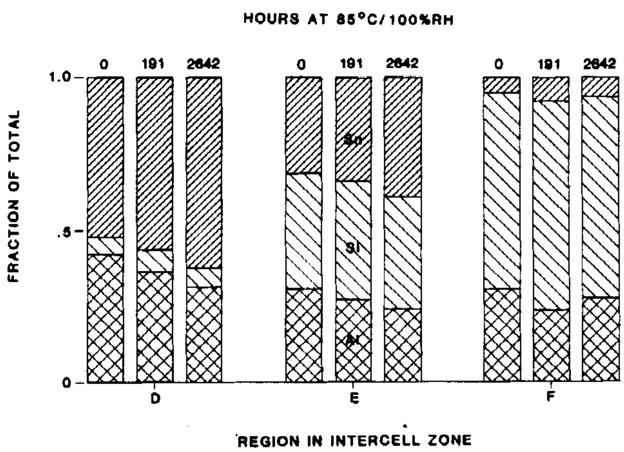

Fig. 6. Elemental Concentration in Intercell Zone of a-Si Module

But the photograph in Fig. 7 clearly attests to the effectiveness of encapsulation in preventing gross regional material losses. The speculation is that the process scribe lines provide ready access to the intercell zone for moisture entering the module at its edges. Additional features of the data (Fig. 8) include a distinct response profile--an initial increase in resistivity followed by a long period of constancy--and a clear differentiation of response to 85% and 100% humidity environments.

A large quantity of light and dark I-V curve numerical data were generated for Batch 1 - 4 samples, including series resistance, power output, and open circuit voltage versus time. Observed trends were as expected: for unencapsulated modules, series resistance values tended to increase and maximum power output tended to decrease with time of exposure by about a factor of 2 in 2000 hours of exposure at 85°C/100%RH; no significant changes in these parameters were observed for encapsulated modules undergoing the same exposure.

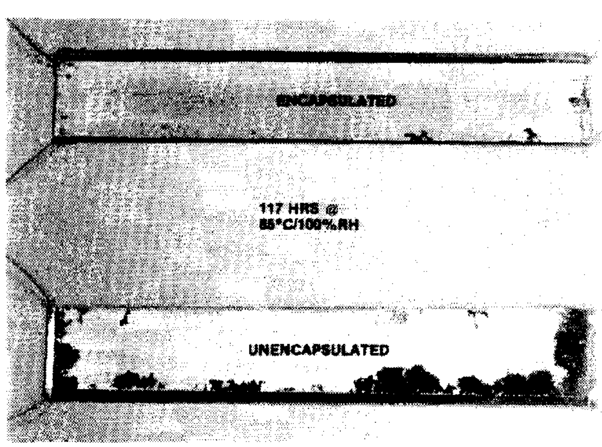

Fig. 7. Material Loss from Fully-Aluminized Back-Surface Modules

Open circuit voltage did not change significantly for EVA-encapsulated modules. A 5-10% reduction was observed after 2000 hours of exposure for unencapsulated modules, a no more serious change than was reported by Lathrop[7] after 2000 hours of exposure at 140°C.

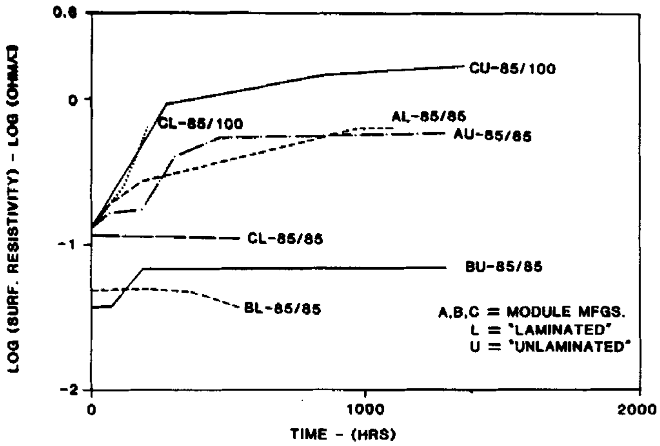

Fig. 8. Back-Surface Resistivity vs. Exposure Time

Lathrop attributed decreases in open circuit voltage and reductions in maximum power output to shunt resistance decreases presumed to result from diffusion of aluminum metallization into the a-Si layers. This particular mechanism was not observed in these experiments, possibly because that alleged diffusion occurs too slowly at 85°C to cause degradation before the pinhole interfusion and stress corrosion cracking mechanisms erode away the aluminum. In other words, the moisture-induced degradation mechanisms described here occur at a much greater rate than the temperature-dependent diffusion degradation mechanism suggested by Lathrop.

It was visually apparent that forward biased, unencapsulated modules suffered a greater degree of corrosion than their unbiased counterparts. For these modules, gathering credible series resistance data proved difficult. Accessing the series resistance region of the I-V characteristic required larger voltage and current levels with each measurement. At the higher voltage levels, the modules could not sustain the required currents. Thus, quantitative differentiation of corrosion/erosion degradation and Staebler-Wronski effect was not achieved.

CONCERNS AND CONCLUSIONS

Moisture will enter and degrade even well-sealed glass-glass modules. At present no technique for preventing this type of degradation, short of hermetic sealing, is known. Low moisture absorbing/retaining encapsulants are recommended.

Annealing a-Si modules prior to installation may stress-relieve the aluminum in the critically important intercell zone and reduce the likelihood of the occurance of these types of erosion.

REFERENCES

1. D.L. Staebler and C.R. Wronski, Appl. Phys. Lett. 31, 292 (1977).
2. D.L. Staebler, IEEE Trans. on Reliability, v. R-31, No. 3, 281-284, August 1982.

3. G. Mon, J. Orehotsky, R. Ross, Jr., G. Whitla, Proceedings of the 17th IEEE Photovoltaic Specialists Conference, 682-692, May 1984.
4. G. Mon, G. Whitla, R. Ross, Jr., M. Neff, IEEE Transactions on Electrical Insulation, v. EI-20, No. 6, 989-996, December 1985.
5. G. Mon, R. Ross, Jr., Proceedings of the 18th IEEE Photovoltaic Specialists Conference, 1142-1149, October 1985.
6. G. Mon, L. Wen, R. Ross, Jr., D. Adent, Proceedings of the 18th IEEE Photovoltaic Specialists Conference, 1179-1185, October 1985.
7. J. Lathrop, 2nd International Photovoltaic Science and Engineering Conference, Beijing, China, August 1986.
8. R. Ross, Jr., 2nd International Photovoltaic Science and Engineering Conference, Beijing, China, August 1986.
9. H. Uhlig, Corrosion and Corrosion Control (Wiley, New York, 1963), pp. 219-222.

This paper presents the results of one phase of research conducted at the Jet Propulsion Laboratory, California Institute of Technology, for the U.S. Department of Energy through an agreement with the National Aeronautics and Space Administration.